

Fabrication of single nanofluidic channels in poly(methylmethacrylate) films via focused-ion beam milling for use as molecular gates

Donald M. Cannon, Jr., Bruce R. Flachsbarth, Mark A. Shannon, Jonathan V. Sweedler,^{a)} and Paul W. Bohn^{b)}

Department of Chemistry, Frederick Seitz Materials Research Laboratory, Department of Mechanical and Industrial Engineering and Beckman Institute for Advanced Science and Technology, University of Illinois at Urbana-Champaign, 600 South Mathews Avenue, Urbana, Illinois 61801

(Received 9 April 2004; accepted 12 June 2004)

Focused-ion beam (FIB) milling provides rapid fabrication of individual cylindrical submicrometer channels with reproducible dimensions ($\pm 5\%$ diameters) through $8\text{-}\mu\text{m}$ thick poly(methylmethacrylate) (PMMA) films. PMMA films are spin-cast on sacrificial Si carriers and sputter-coated with Au before the 30-kV gallium FIB milling process. By adding a trace amount of poly(ethyleneoxide) and poly(dimethylsiloxane) to the PMMA solution before casting, the films can be released for subsequent mounting in microfluidic devices to create hybrid microfluidic-nanofluidic multilevel architectures. *In situ* FIB sectioning demonstrates the smooth cylindrical surface within the pore. Placing a milled film in contact with an aqueous fluorescein solution fills the channel by capillary action, as verified by confocal fluorescence microscopy. Confocal fluorescence of dyed films reveals that the pores span the thickness of the PMMA film. Small arrays of channels with a defined number and density and arbitrary in-plane spatial arrangement are fabricated with this process, allowing a unique testbed for high aspect ratio nanofluidic devices. © 2004 American Institute of Physics. [DOI: 10.1063/1.1780605]

Miniaturizing analytical techniques through the use of microfluidics enables enhanced analysis and sensing through lab-on-a-chip strategies. In this context, nanofluidics, in which fluids are pumped in capillaries of nanometer characteristic dimensions, is of interest due to the small volumes, high surface-to-volume ratios and novel transport phenomena.^{1,2} Nanofluidics has been applied to single-molecule sensing,³ chemical separations,^{4,5} microfluidic interconnects,^{6,7} and fundamental studies of fluid transport at nanometer dimensions.^{8,9} Single molecule detection through supported α -hemolysin nanopores³ has shown such promise that synthetic nanopore analogs are now being aggressively pursued through a variety of fabrication techniques,^{10–12} including microfabrication,¹³ nanoscale templates,¹⁴ nanoprinting,¹⁵ and nuclear track etching.¹⁶ Particular interest is focused on the study of single pores, because (a) ensemble measurements yield statistical averages, missing outliers; (b) different pores have different physical and chemical properties; and (c) single pores can be fabricated to specific design rules and thoroughly characterized.

Focused-ion beam (FIB) milling and assisted deposition is commonly used as a sub-micrometer fabrication tool¹⁷ but has traditionally not been used for insulating substrates. Poly(methylmethacrylate), PMMA, a well-known electron beam resist,¹⁸ is interesting in this regard due to its unusually high ion-beam sputtering yield, allowing facile creation of polymer gratings,¹⁹ masters for high-resolution elastomer molding,²⁰ and patterned resists for anodic alumina etching.²¹ Our interest in controlling molecular transport within submicrometer-sized structures led us to pursue FIB

milling through thin films of PMMA as a route to the fabrication of individual submicrometer channels, because they exhibit large aspect ratios and the fabrication control necessary to create spatially defined arrays of submicrometer channels.

PMMA films (1:1:5 weight ratio of 350 kDa PMMA: methylmethacrylate:anisole) were spin-cast (6000 rpm, $\sim 8\text{-}\mu\text{m}$ thick) on $5\text{ mm} \times 5\text{ mm}$ Si wafers and cured at $195\text{ }^\circ\text{C}$ for $\geq 1\text{ h}$. A small ($< 1\%$) amount of poly(ethyleneoxide)/poly(dimethylsiloxane) copolymer added prior to casting allowed the PMMA films to be released from the underlying Si carrier. Au sputter coating was necessary to reduce charging artifacts during FIB milling or SEM monitoring, with Au films $> 10\text{ nm}$ thick exhibiting minimal residual damage at low current. After milling, the PMMA film was removed from the Si carrier and mounted in a multilevel microfluidic structure.¹ The $8\text{-}\mu\text{m}$ thickness was chosen as a compromise between the time needed to mill the pore and achieving sufficient rigidity to allow the released films to be handled easily. The FIB instrument (FEI Strata Dual Beam 235) was optimized for milling through a non-conductive material. Spot-mode, in which the rastering ion-optics are decoupled from the focused-ion beam, with location and duration being computer controlled, provided the most reproducible and smallest diameter channels with minimal residual damage.

A 1-pA aperture produces pore diameters, d_p , between $75\text{ nm} < d_p < 110\text{ nm}$, while the 50-pA aperture results in diameters between $300\text{ nm} < d_p < 400\text{ nm}$. The minimum diameters obtainable are determined by the aperture size when instrumental alignment parameters are optimized. The channel diameters, however, are larger than expected based on the current aperture. Pore widening is attributed to secondary electron damage and effects, such as substrate heating that accompany 30-kV ion bombardment of a nonconductive sub-

^{a)} Author to whom correspondence should be addressed; electronic mail: sweedler@scs.uiuc.edu

^{b)} Author to whom correspondence should be addressed; electronic mail: bohn@scs.uiuc.edu

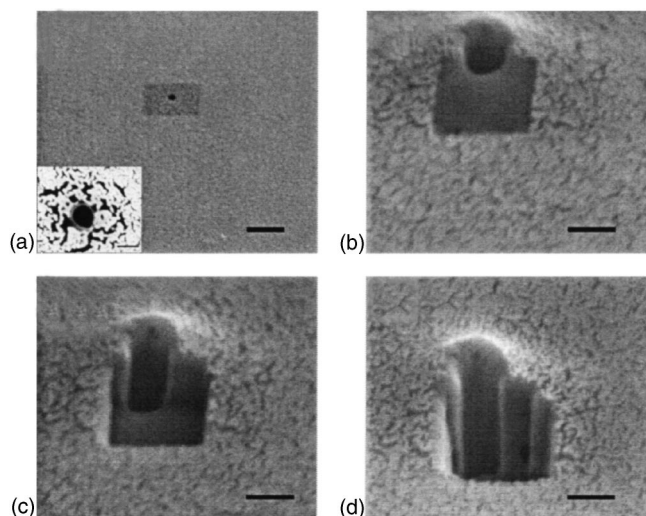


FIG. 1. FIB sectioning applied to dimensional profiling. (a) Original pore; scale bar $2\ \mu\text{m}$. (Inset) Single channel fabricated by FIB (1-pA aperture), showing the damage pattern around the mouth of the channel; scale bar $200\ \text{nm}$. (b)–(d) Original pore overlaid with rectangular milled volume successively exposing larger portions of the pore; scale bar $500\ \text{nm}$. Scanning electron micrographs (5-kV, 52° viewing angle) were collected by briefly halting the ion beam sectioning process.

strate. These damage effects are evident in the patterning of the Au sputtered layer directly around the mouth of the milled pore, cf. Fig. 1(a), inset. Additionally, SEM energies must be kept low (1–5 kV) for *in situ* characterization of the nascent structures, because areas imaged with 15-kV and higher energy electrons routinely show field-of-view damage as depressed areas. Single channels are completely milled through the $\sim 8\text{-}\mu\text{m}$ thick PMMA layer in $\approx 3\ \text{s}$. Exposure of the growing pore to the ion beam for longer times produces larger diameters and elliptical pore cross sections, which are postulated to arise from ion-beam shift effects that occur when the ion beam encounters the underlying Si–PMMA interface.

Dimensional uniformity is critical for investigating molecular transport through these structures. Using the dual functions of the FIB/SEM instrument, channels can be dimensionally profiled directly after milling, viz. Fig. 1, by rastering the ion beam in a square intersecting the midpoint of the pores, effectively providing a cross-sectional image down the length of the channel. Clearly the channel exhibits excellent cross-sectional uniformity along its length. Tapering of the diameter, an effect observed in submicrometer pores produced by nuclear track etching,²² is not observed. All pores examined in this manner show smooth nontapered interior surfaces, which are advantageous for electrokinetic fluid transport applications.

Confocal fluorescence microscopy (Leica Microsystems SP2) was also used to investigate the larger diameter channels. Soaking the PMMA layer in a *t*-butanol solution containing rhodamine dye results in rapid incorporation of the dye throughout the polymer, permitting negative tone fluorescent sectioning by confocal microscopy. The cross section shown in Fig. 2(a) was obtained by carefully aligning the xz plane of the confocal image with the longitudinal axis of the pore. The single pore spans the $8\text{-}\mu\text{m}$ thick PMMA film, illustrating the uniform diameter along the length of the pore, the high aspect ratio (~ 20 for the pore shown), and confirming that the time required to mill through $8\text{-}\mu\text{m}$ PMMA lay-

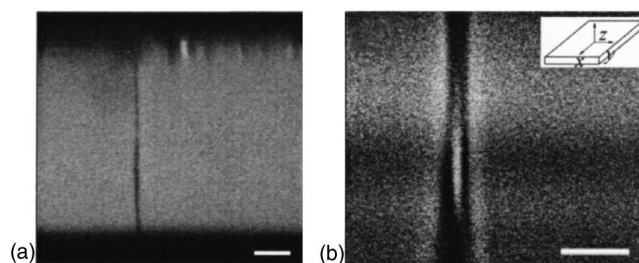


FIG. 2. Confocal fluorescence image sectioning parallel to the xz plane. (a) Vertical slice through a dyed-PMMA layer with a single pore spanning the layer; scale bar $2\ \mu\text{m}$. Measured diameter= $400\pm 35\ \text{nm}$ ($n=10$). (b) Vertical slice through a dye-filled pore; scale bar $8\ \mu\text{m}$. (Inset) Coordinate system for confocal imaging.

er is less than 3 s. Figure 2(b) shows an xz section through a pore within which a $1\ \mu\text{M}$ aqueous fluorescein solution is being transported, illustrating the high sensitivity of confocal fluorescence imaging and raising the possibility of studying transport in the interior of single pores by confocal sectioning.

Finally, the dimensional reproducibility combined with the specific location control of the FIB also allows the creation of arrays of submicrometer channels with defined number and density. Figure 3(a) shows an xy slice from the center of a dual pore PMMA film in contact with $10\ \mu\text{M}$ aqueous fluorescein. The $\sim 600\ \text{nm}$ measured diameter of the fluorescent spots matches the pore diameters measured by SEM to within $\pm 20\%$. The clear spatial isolation of dye solution in the adjacent nanopores, evident in Fig. 3(a), results from the fact that aqueous fluorophore solutions do not intercalate into the PMMA layer, even upon extended soaking. A demonstration of the direct-write capabilities of FIB to produce high precision arrays of submicrometer channels with arbitrary control over spatial alignment is shown in Fig. 3(b). This array is characterized by $\sim 5\%$ standard deviation for the horizontal diameters, $d=170\pm 10\ \text{nm}$; $n=26$. Controlling the number and spatial placement of multiple channels is a powerful tool for investigating electrokinetic transport at the nanoscale.

In summary, FIB has been exploited for rapid direct-writing of uniform cylindrical submicrometer pores in PMMA, either as single channels, or as spatially defined small-area arrays. The fabricated pores have been characterized by electron microscopy and by confocal fluorescence sectioning. In contrast to statistical methods of preparing ensembles of submicrometer pores, FIB through-layer milling

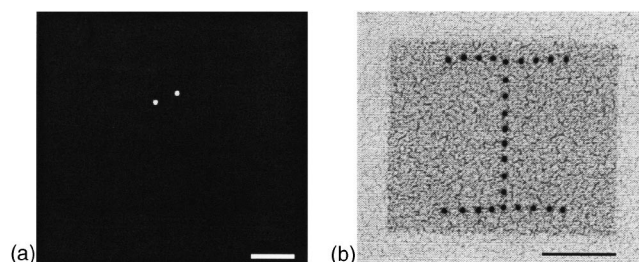


FIG. 3. (a) Confocal fluorescence image of two dye-filled pores, showing an xy plane at a z position approximately at the center of the PMMA layer; scale bar $4\ \mu\text{m}$. Measured fluorescent spot diameter is $\approx 600\ \text{nm}$. (b) SEM image of a patterned array of submicrometer pores. Each milling location was positioned via a computer generated graphical image overlay. 1-kV SEM image. Pore diameter= $170\pm 10\ \text{nm}$ ($n=26$); scale bar $2\ \mu\text{m}$.

produces highly uniform pores and allows excellent control over both geometry and placement of channels, thus, rendering this approach useful for molecular delivery and sensor applications. Studying single pores should also lead to better understanding of nanoscale transport phenomena, allowing more efficient utilization of nanoscale fluidic components in many disciplines.

This research was supported by the Department of Energy under Grant No. FG0288ER13949, the National Science Foundation through the Center for Advanced Materials for Water Purification, and the National Institute for Allergies and Infectious Diseases through the Great Lakes Regional Center of Excellence. D.M.C. acknowledges the Arnold and Mabel Beckman Foundation Postdoctoral Fellows Program. FIB milling was carried out in the Center for Microanalysis of Materials, University of Illinois, which is partially supported by the U.S. Department of Energy under Grant No. DEFG02-91-ER45439.

- ¹T.-C. Kuo, L. A. Sloan, J. V. Sweedler, and P. W. Bohn, *Langmuir* **17**, 6298 (2002).
²P. J. Kemery, J. K. Steehler, and P. W. Bohn, *Langmuir* **14**, 2884 (1998).
³J. J. Nakane, M. Akeson, and A. Marziali, *J. Phys.: Condens. Matter* **15**, R1365 (2003).
⁴M. Nishizawa, V. P. Menon, and C. R. Martin, *Science* **268**, 700 (1995).
⁵L. A. Woods, T. P. Roddy, T. L. Paxon, and A. G. Ewing, *Anal. Chem.* **73**,

- 3687 (2001).
⁶T.-C. Kuo, D. M. Cannon, Jr., Y. Chen, J. J. Tulock, M. A. Shannon, J. V. Sweedler, and P. W. Bohn, *Anal. Chem.* **75**, 1861 (2003).
⁷D. M. Cannon, Jr., T.-C. Kuo, P. W. Bohn, and J. V. Sweedler, *Anal. Chem.* **75**, 2224 (2003).
⁸A. T. Conlisk, J. McFerran, Z. Zheng, and D. Hansford, *Anal. Chem.* **74**, 2139 (2002).
⁹R. Qiao and N. R. Aluru, *Nano Lett.* **3**, 1013 (2003).
¹⁰J. Li, D. Stein, C. McMullan, D. Branton, M. J. Aziz, and J. A. Golovchenko, *Nature (London)* **412**, 166 (2001).
¹¹J. P. Alarie, A. B. Hmelo, S. C. Jacobson, A. P. Baddorf, L. Feldman, and J. M. Ramsey, *Fabrication and Evaluation of 2D Confined Nanochannels in Micro Total Analysis Systems*, Squaw Valley, CA, 2003, Vol. 1, edited by K. F. Jensen and D. J. Harrison (Transducers Research Foundation, Cleveland Heights, Ohio), p. 9.
¹²H. D. Tong, H. V. Jansen, V. J. Gadgil, C. G. Bostan, E. Berenschot, C. J. M. van Rijn, and M. Elwenspoek, *Nano Lett.* **4**, 283 (2004).
¹³J. Han and H. G. Craighead, *Science* **288**, 1026 (2000).
¹⁴L. Sun and R. M. Crooks, *J. Am. Chem. Soc.* **122**, 12340 (2000).
¹⁵O. A. Saleh and L. L. Sohn, *Nano Lett.* **3**, 37 (2003).
¹⁶C. C. Harrell, S. B. Lee, and C. R. Martin, *Anal. Chem.* **75**, 6861 (2003).
¹⁷S. Rennon, L. Bach, H. Konig, J. P. Reithmaier, A. Forchel, J. L. Gentner, and L. Goldstein, *Microelectron. Eng.* **57–58**, 891 (2001).
¹⁸E. A. Dobisz, S. L. Brandow, R. Bass, and J. Mitterender, *J. Vac. Sci. Technol. B* **18**, 107 (2000).
¹⁹C. Aubry, T. Trigaud, J. P. Moliton, and D. Chiron, *Synth. Met.* **127**, 307 (2002).
²⁰N. W. Liu, A. Datta, C. Y. Liu, and Y. L. Wang, *Appl. Phys. Lett.* **82**, 1281 (2003).
²¹Y. Liu, D. M. Longo, and R. Hull, *Appl. Phys. Lett.* **82**, 346 (2003).
²²J. C. Hulthen and C. R. Martin, *J. Mater. Chem.* **7**, 1075 (1997).